# Detection and Classification of Soft Exudates in Retinal Fundus Images

*Image Processing and Analysis*

*A. Cartaya, M. Rivas, E. Castrechini, D. Gonzalez, E. Matamoros*
*University of Cassino and Southern Lazio, Cassino, Italy.*
*June 2023*

## Introduction

Accurate detection of soft exudates (SEx) in fundus retinal images is crucial for the early diagnosis of diabetic retinopathy. However, the detection process faces several challenges, including variability in appearance, similarity to other retinal features, low contrast, and the presence of noise and artifacts. A method for detecting these lesions was proposed based on the characteristics mentioned in the following section.

### Characteristics of SEx used as the basis for the algorithm

1. Soft exudates generally exhibit higher intensity compared to the surrounding areas [1].
2. They lack well-defined borders [2].
3. They display significant variability in terms of size and shape [3].
4. Soft exudates are typically confined to the posterior segment of the fundus, and their size rarely surpasses one-third of the optic disc area [4].

### Algorithm Pipeline

Based on the four aforementioned characteristics, a model was developed to automate the detection of soft exudates. The model consists of four main steps:

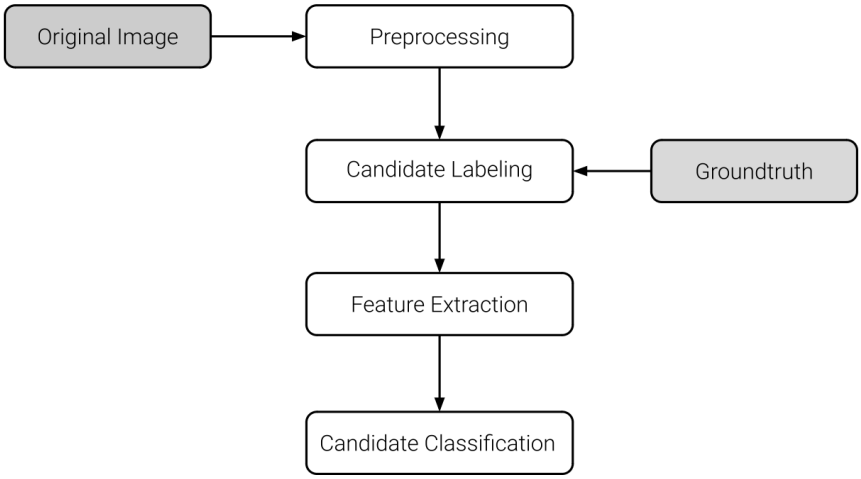


*Figure 1: Proposed Methodology for Exudate Detection*

## *Preprocessing*

The implemented preprocessing is based on two sequential segmentations:

### Basic Segmentation

In this part, a non-rigorous segmentation of the soft exudates is attempted, taking into account the four basic characteristics mentioned earlier. The result is a series of basic candidate contours (BCC). The primary objective of this part is to maximize the number of detected lesions (increase sensitivity), while ensuring that the candidate contours containing lesions are of appropriate size and that the lesions are centered within the bounding boxes of the contours. See to *Fig. 2A*.

### Advanced Segmentation

After obtaining the BCC, the attention is directed towards each of them to obtain advanced candidate contours (ACC) that closely resemble the true shape and size of the lesion, increasing the Intersection over Union (IoU). In this advanced segmentation, the bounding box of each BCC is taken and enlarged by a scale factor based on the area of the BCC. The new bounding boxes become the new regions of interest (ROIs). Subsequently, individual preprocessing is applied to each ROI to enhance the lesion and achieve a more precise segmentation. See to *Fig. 2B*.

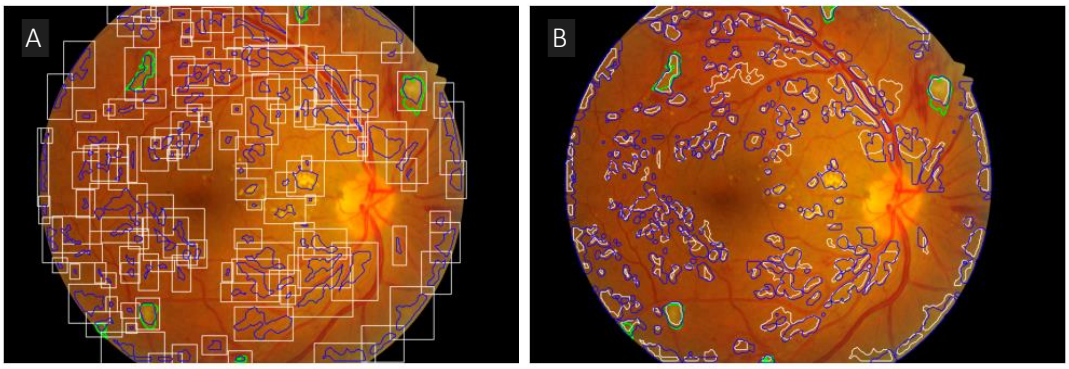


*Figure 2: Original image with the BCC (blue) and the enlarged bounding boxes (white) (A) and the ACC (blue) over the BCC (white) (B) Groundtruths in green*

## *Candidate Labelling*

After detecting the candidates, a labelling process was performed to differentiate between the actual lesions, referred to as True Positives (TP), and those that did not correspond to real lesions, known as False Positives (FP).
This labelling was based on the IoU with the groundtruths.
This step was carried out to train a machine learning model to distinguish between real lesions and false ones among the candidates.

## *Feature Extraction*

Once the candidates were labelled the feature extraction was performed. This step focuses on extracting relevant features from the identified regions of interest (ROIs). To accomplish this, a method incorporating the ROIs enhancement and the acquisition of different types of features was employed.

## *Report Organization*

The following sections are organized as follows: I – Basic Segmentation II – Advanced Segmentation III – Candidate Labelling IV – Feature Extraction V – Feature Classification VI – Results VII – Annexes.

# I - Basic Segmentation

A preliminary basic segmentation was performed to obtain a series of BCC characterized by not being extremely large or small, and by attempting to center the lesions within their bounding box. This segmentation is based on the following steps: 1) Preprocessing of the entire image, 2) subdivision of the image into blocks to work with smaller regions, 3) reconstruction of the image from the preprocessed blocks, 4) separation of large contours and filtering based on shapes and sizes, 5) obtaining final contours and scaled bounding boxes. Each step of the basic segmentation is explained in detail below.

## 1) Preprocessing of the entire image

*First, the entire image was preprocessed to enhance the lesions (See Fig. 3).*

### *Step 1: Remove the Optical Disk region enlarged by a factor of 1.5*

Based on the 4th basic characteristic of soft exudates, the region of the optical disk (OD) enlarged by a factor of 1.5 was removed from the original image (see *Annex 1*). This was done because the OD region is naturally the brightest region of the fundus image and can distort the following steps that are based on the 1st basic characteristic of soft exudates.

### *Step 1.2: Reduce the image by a scale factor of 0.1*

Once the OD region was segmented, the image was reduced by a scale factor of 0.1 (10% of the original image). This was mainly done to speed up the preprocessing, and the scale factor was chosen to preserve the lesion details.

### *Step 2: Extract the green channel*

Since soft exudates exhibit high contrast in the green channel, the second channel (corresponding to green) of the image was extracted and further processing was carried out using only this channel.

### *Step 3: Apply CLAHE*

Next, Contrast Limited Adaptive Histogram Equalization (CLAHE) was applied to enhance contrast while limiting noise amplification. The clip limit chosen was 14, which adequately highlighted the bright regions while adding minimal noise. The window size was left as the default (8x8).

### *Step 4: Apply Median blur*

A Median blur filter with a kernel size of 3 was applied to reduce noise in the image (including noise introduced by the previous histogram equalization). A kernel size of 3 was chosen to preserve information about smaller lesions.

### *Step 5: Apply Gamma correction*

Gamma correction with a sigma value of 2 was applied to enhance the brightness of brighter areas and darken the darker areas of the image.

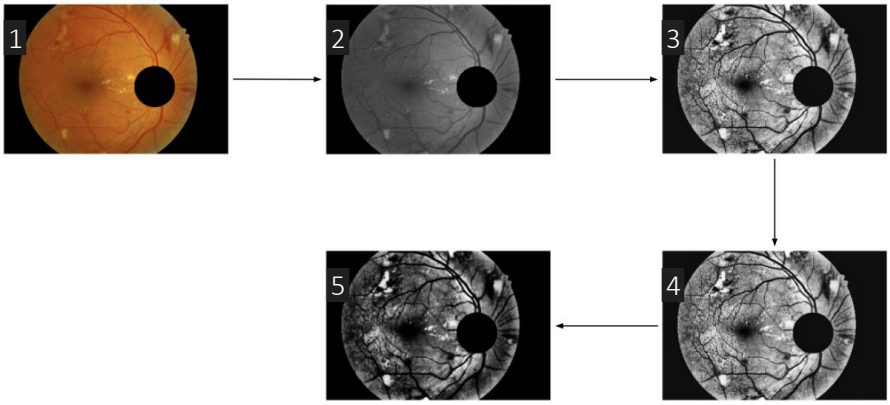


*Figure 3: Image after applying each one of the basic segmentation steps*

## 2) Subdivision into blocks to work with smaller regions

*Once the lesions were enhanced, the image was divided into equally sized regions to work with them individually and highlight potential candidates within them (See Fig. 4).*

### *Step 6: Add padding to the image and then subdivide into tiles*

First, zero padding of size (31 x 27) was added to the bottom and right of the image to allow for subdivision into 35 x 35 regions. The size of the region was chosen based on the bounding box of the largest soft exudate in the training dataset. Each region was then processed individually.

### *Step 7: Apply Gaussian blur*

A Gaussian blur filter with a window size of 5x5 was applied to each region to blur the edges of bright regions and enhance their centers.

### *Step 8: Apply Gamma correction*

A stronger gamma correction with a sigma value of 3.3 was applied to each region to further enhance the brighter parts.

### *Step 9: Apply Otsu threshold*

Finally, a binary threshold was applied to each region using Otsu's method to obtain an optimal threshold value.

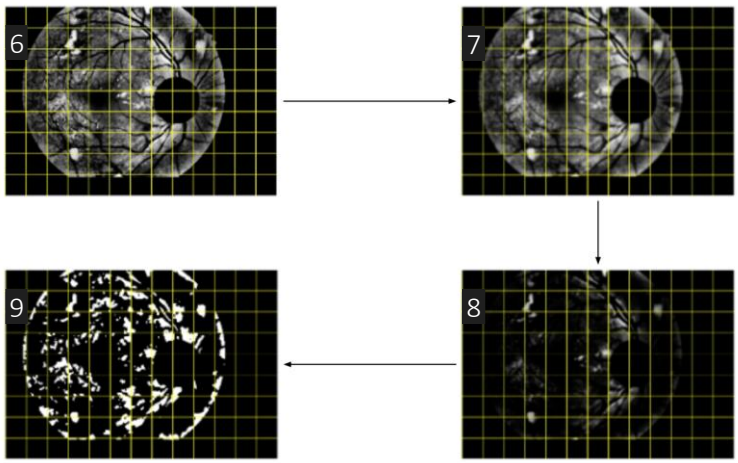


*Figure 4: Image after applying each one of the block preprocessing steps*

## 3) Reconstruction of the image from the preprocessed blocks

After binarizing each region, the image was reconstructed to its original size. This was done by placing each region in its corresponding position and removing the added padding.

## 4) Obtaining contours and filtering based on shapes and sizes

### *Steps 10-12: Sequential filter for breaking big elements*

Once the image was reconstructed, contours were sought that met the characteristics mentioned earlier, i.e., contours that were neither extremely small nor extremely large. To achieve this, a series of sequential filters were applied based on the following steps:

- Contours were obtained from the binary image.
- Contours smaller than a threshold ($size\_th$) were saved in a list ($small\_elements$).
- An opening operation was applied using a circular structuring element (SE) with a radius ($se$).
- The contours saved in $small\_elements$ were drawn back on the opened image image.

This process was repeated three times with $size\_th = [300, 300, 400]$ and $se = [7, 7, 10]$. These sequential filters were designed to break down very large contours formed by small or medium regions connected by a small group of pixels. This is achieved thanks to the applied openings. However, applying openings may modify or eliminate some medium or small contours, so they were saved in a list and redrawn on the opened image.

### *Step 13: Connecting small elements*

After working separately on large elements, the small elements were connected. This was achieved by applying a closing operation with a circular structuring element of radius 3. A smaller radius was chosen compared to the previous step to avoid undoing the destruction of large contours.

### *Step 14: Filter small elements*

Contours with an area smaller than 3 were removed since they were either some residues of steps 10-12 or simply noise in the image.

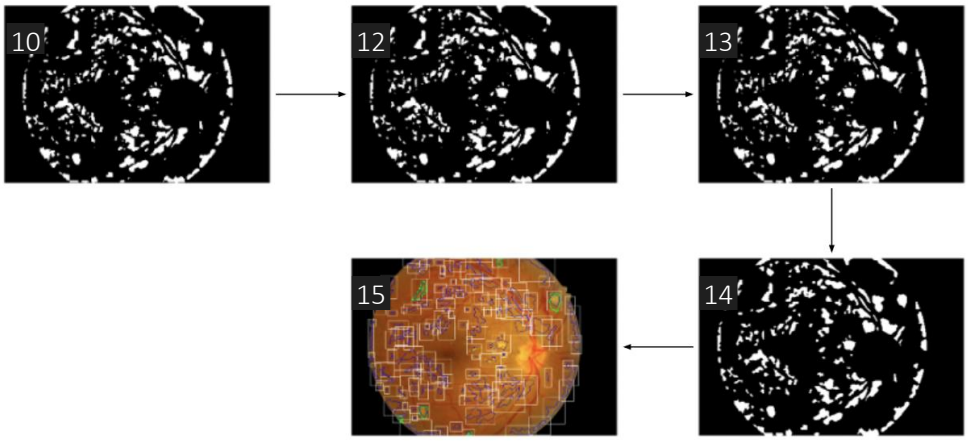


*Figure 5: Image in the steps 10-14 and the result of the basic segmentation*

## 5) Obtaining final contours and scaled bounding boxes

Finally, the resulting contours from the previous step were obtained along with their corresponding bounding boxes. These bounding boxes were scaled based on the area of the enclosed contour. This approach was adopted because, in some cases (mostly when the area of the contour was small), the

bounding box did not fully contain the actual lesion. The scale factors for the bounding boxes with respect to the contour areas were as follows:

| Area | Bounding box scale factor |
|---|---|
| $\leq 30$ | 1.7 |
| $\leq 50$ | 1.6 |
| $\leq 100$ | 1.4 |
| $\leq 150$ | 1.3 |
| $\leq 300$ | 1.2 |
| $\leq 400$ | 1.1 |
| $> 400$ | 1 |

*Table 1: Area of the enclosed contour and the scaling factor applied to the bounding box*

Finally, the BCC and their corresponding dilated bounding boxes were obtained. These were mapped to the original image size by multiplying them by a factor of $10 = \frac{1}{0.1}$.

# II - Advanced Segmentation

Once the BCC and scaled bounding boxes were obtained, the next step was to work with these bounding boxes as Regions of Interest (ROIs) in the original image to approach the true shapes of the SEx possibly contained within the ROIs. This advanced segmentation is based on the following steps: 1) preprocessing of the entire image, 2) ROI-based preprocessing, 3) reconstruction of the original image from the preprocessed ROIs, 4) global and individual contour dilation and filtering.

## 1) Preprocessing

*First, the entire image was preprocessed to enhance the lesions (See Fig. 6).*

### *Step 1: Remove OD*

Similar to the basic segmentation, the optical disk (OD) was removed, but this time more precisely using the advanced optic disk segmentation (see *Annex 2*).

### *Step 1.2: Reduce the image by a scale factor of 0.4*

After inspecting results at multiple scales, it was found that the original image (4000 x 2000) does not provide a noticeable change compared to lower-resolution images (>30% of the original image) when segmenting SEx. This is because, despite the reduction in size, SEx with their not well-defined edges do not lose any fine details in the transformation. This reduction in size also helps reduce the considerable amount of noise in the original image and speeds up the processing of the subsequent steps. The chosen scaling factor was 0.4 (40% of the original image).

### *Step 2-5: Preprocessing of the entire image*

Similar to the basic segmentation, the entire image underwent preprocessing to enhance the lesions. The following steps were applied: CLAHE with clip = 14, Median blur with a kernel size of 3, and Gamma correction with a sigma value of 2.

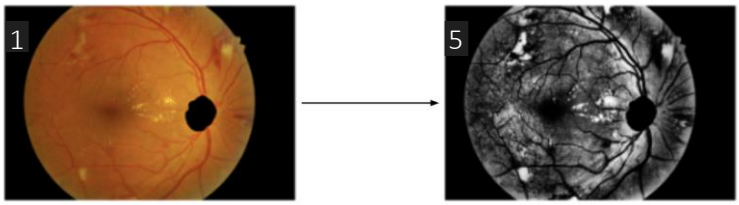


*Figure 6: Original image after the advance OD removal and the preprocessing*

# 2) ROI-based processing:

## *Step 6: Work with each ROI independently*

Next, each ROI obtained from the basic segmentation was processed individually (See Fig. 7).

## *Step 7: Preprocess the entire image depending on the ROI mean intensity*

In this step, the mean intensity of each ROI was calculated. Then, the entire image was preprocessed again in function to the mean intensity of the ROI. This adjustment modified the parameters of CLAHE ($clahe\_clip$) and Gamma correction ($sigma$) as follows:

- If the mean intensity is less than or equal to 34, $\text{clahe\_gamma} = 66$.
- If the mean intensity is less than or equal to 130, $\text{clahe\_gamma} = -0.4 * \text{mean\_intensity} + 90$.
- Otherwise, $\text{clahe\_gamma} = 35$.

Where:

- $clahe\_clip = clahe\_gamma$
- $sigma = \frac{clahe\_gamma}{100}$

These values were obtained by performing a linear regression (with saturation points) of the $\text{clahe\_gamma}$ with respect to the "quality" of the lesion segmentation (the "quality" was evaluated manually with the help of two track bars and a lot of patience inspecting all the images of the training set). Five points were used to create the linear function:

- The point with the minimum intensity ($0^{th}$ percentile).
- The $25^{th}$ percentile.
- The $50^{th}$ percentile.
- The $75^{th}$ percentile.
- The point with the maximum intensity ($100^{th}$ percentile).

The idea behind this method come from the hypothesis that by preprocessing the entire image based on the intensity of a single region, the preprocessing highlights the specific region, considering the neighboring regions. Once the entire image is preprocessed with respect to the ROI, the region is segmented and processed individually.

## *Step 8-10: Preprocessing of ROIs*

Similar to steps 7-9 of the basic detection, each ROI was processed separately. Median blur with a window size of 15x15, Gamma correction with $sigma = 4.17$, and a binary threshold with Otsu's method were used.

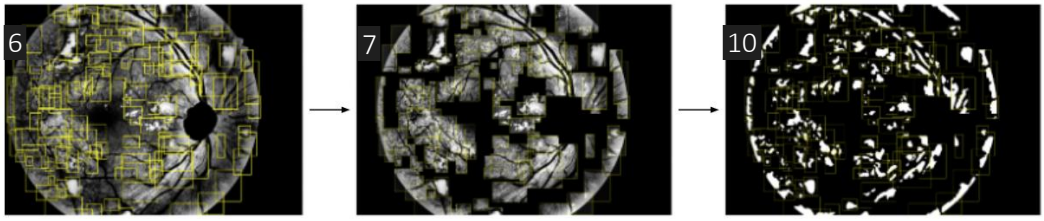


*Figure 7: Main steps of the ROI-based preprocessing*

## 3) Reconstruction of the original image from the processed ROIs

Once all the ROIs were processed, the image was reconstructed. To address the issue of overlapping (since some bounding boxes overlap with neighboring regions), the contours were drawn one by one on top of a black background. An $OR$ function was applied when drawing the new contours on top of the previous ones.

## 4) Global and individual contour dilation and filtering

### *Step 11: Global dilation*

After reconstructing the image, a global dilation was applied to the entire image using a circular structuring element (SE) with a radius of 7. This dilation was used because, due to the high sigma values in the gamma correction, some lesion contours became very small after thresholding. The global dilation helps restore part of their original size, moreover, assists in connecting small and nearby regions to form new candidates (possible SEx due to density).

### *Step 12: Individual dilation*

After applying the global dilation, each contour was dilated individually. This serves to further increase their size without the risk of merging and creating a larger contour. The process involves:

- Drawing each contour on a black image of the same size as the actual image.
- Dilating the drawn contour.
- Saving the new dilated contour.

A circular kernel with a radius of 3 was chosen for the dilation. A smaller kernel was used to avoid excessive overlapping that could cause a lesion to belong to two different contours. Once this individual dilation is performed, it reaches the "No Binary Point" where the contours cannot be drawn again on a binary image and extracted as multiple contours because many of them will overlap and create a larger contour.

### *Step 13: Resize contours and filter by area*

After the individual dilation, the contours are resized back to their original size by multiplying them by a scale factor of $\frac{1}{0.4}$. Then, the contours are filtered by size, where the low threshold is set to $min\_area * 0.25$ and the high threshold is set to $max\_area * 1.5$. The values for $min\_area$ and $max\_area$ are chosen as follows:

- $min\_area = 773$: area of the smallest SE in the training dataset.
- $max\_area = 54468$: area of the largest SE in the training dataset.

Finally, after filtering the contours, the final Advance Candidates Contours (ACC) are obtained (See Fig. 8).

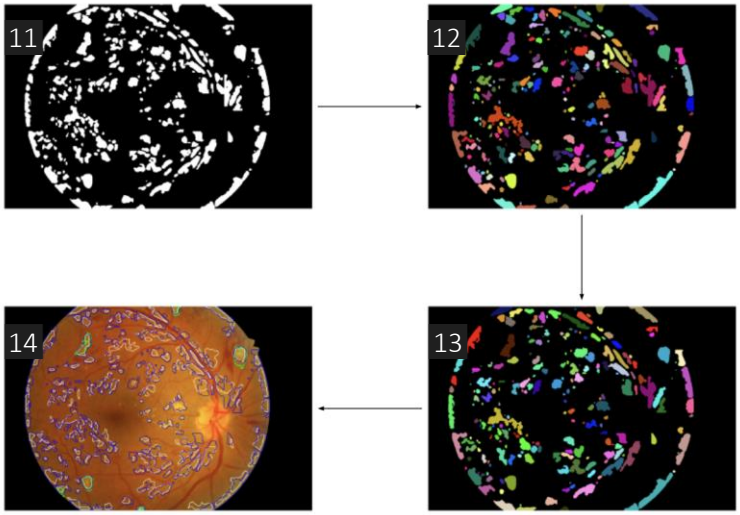


*Figure 8: Global and individual contour dilation, filtering, and the final result of the advanced segmentation*

# III Candidate Labelling

The candidates obtained in the previous step were labeled to differentiate them when training a machine learning model capable of distinguishing between TP ($label = 1$) and FP ($label = 0$). This labelling was performed using the IoU metric.

To be considered TP, the candidates had to have an IoU greater than the established threshold (different values were tested).

The steps followed to label each candidate are as follows:

1. Draw the candidate in a black image
2. Draw a groundtruth contour for that image in a black image
3. Calculate the IoU between them
4. Give the candidate a label:
    a. If the IoU is lower than the established threshold, label the candidate as FP and go back to step 2
    b. If it is higher:
        i. Check if there is another candidate matching the groundtruth contour:
            1. If there is, choose the one with the highest IoU this one will be a TP and the other, FP. Go back to step 2
            2. If there is none, label it as TP and go back to step 2

These steps were followed for all candidates until the labels were saved for each one.

# IV Feature Extraction

## 1) Extract features from ROIs

### *Step 1: Obtaining Bounding Boxes and Contour lists*

Through the segmentation process, the ACC and their corresponding bounding boxes were obtained.

### *Step 2: Creating Contour Masks and Extracting ROIs*

To extract meaningful features from the segmented lesions, the contour mask of the candidates was used to isolate them from the rest of the bounding box, making the features to be focus exclusively on the lesion area.

### *Step 3: ROIs Enhancement*

To improve the classification of the candidates, different enhancements were tried, some of these operations are:

- Converting to grayscale
- Selecting a specific channel (green)
- Median Blur filtering
- Gaussian Blur filtering
- Histogram equalization
- CLAHE
- Denoising
- Normalization

These steps aim to improve the visual quality and prepare the ROI for features extraction.

## 2) Feature Extraction

*Table 2* shows all the features extracted and its type.

| Type of features | Features |
|---|---|
| Texture (52 features) | - Gray-level co-occurrence matrix (GLCM)<br>- Local binary patterns (LBP)<br>- Haralick (from GLCM)<br>- GLRLM features |
| Color (21 features) | Mean and $\sigma$ from each channel in the color space:<br>- RGB<br>- CieLAB<br>- HSV<br>And $\sigma^2$, skewness and kurtosis in grayscale |
| Shape (13 features) | - Area<br>- Perimeter<br>- Circularity<br>- Aspect Ratio<br>- Sodality<br>- Extent<br>- Hu moments |
| Statistical (7 features) | - Fourier descriptors |

*Table 2: Types of features and the ones extracted*

## 3) Feature Normalization

In order to prepare the feature vector for training a Machine Learning algorithm to classify the features, the values in each column of the feature vector were normalized using Min-max scaling. This scaling technique ensures that the features are transformed to a normalized range of [0, 1].

## 4) Feature Selection

The process of feature selection aids in identifying the most informative and relevant features for the given task.

### *First approach (SelectKBest)*

In this approach, the top K features are selected based on statistical scoring methods such as chi-square, ANOVA F-value, or mutual information. SelectKBest proves to be advantageous when there is a large number of features, and the focus is on identifying the most discriminative ones.

### *Second approach (Random Forest)*

This approach employs the Random Forest algorithm to estimate the importance of each feature in the classification process. By training a Random Forest model and analyzing the feature importance, the features can be ranked, and the most relevant ones can be selected. Random Forest-based feature selection offers the advantage of capturing complex interactions and dependencies among features.

# V Results

## Sensitivity

The formula used to calculate sensitivity is as follows: $sensitivity = \frac{TP}{TP+FN}$, where TP represents the number of candidates that match with a lesion in the groundtruths (with an IoU greater than a certain threshold), and FN represents the total number of lesions present in all the groundtruths except those that are detected as TP (See Fig. 9)

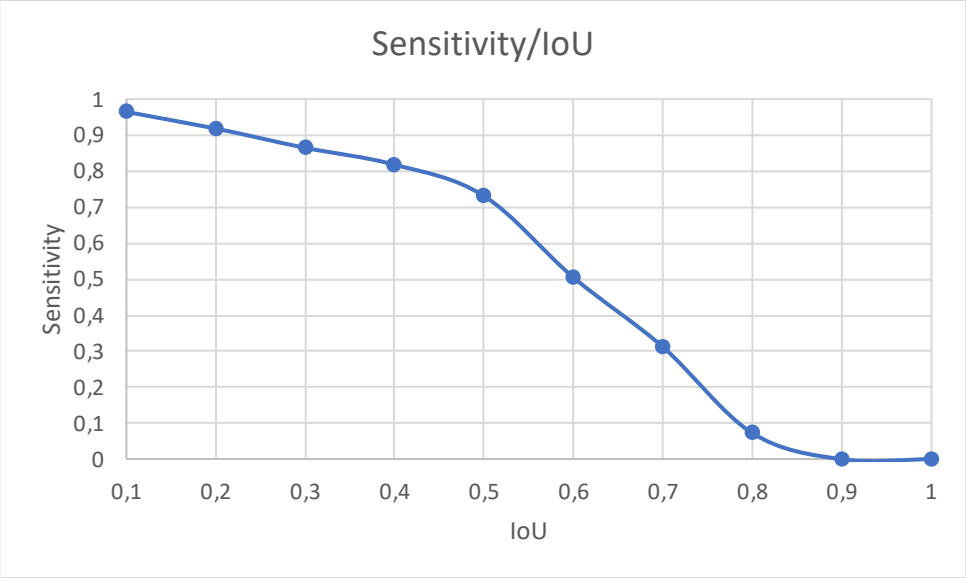


*Figure 9: the graph illustrates the varying sensitivities at different IoU thresholds.*

These results demonstrate that the segmentation of the candidates is highly accurate, as a minimal number of lesions are lost. With an IoU of 0.1, almost none are missed, resulting in a sensitivity approaching 1.

## ROC and Precision-Recall curves

A ROC curve was created in order to estimate the performance of the classifier. This classifier is a SVM created to be able to treat imbalanced data (in the candidates list there are much more False Positives than True Positives 1:121). Based on the graph, it is evident that the classification performance is suboptimal. In order to enhance the classifier's performance, it is necessary to improve or select additional features.

The precision-recall curve was plotted to show the full performance of the algorithm, using the Area Under the Curve Precision-Recall (AUCPR), being the ideal performance an $AUCPR = 1$. In this curve it is possible to see the performance of the segmentation and the classification together.
Despite achieving a good segmentation with a high sensitivity, the results indicate poor classification performance. This suggests that there is room for improvement in the classification process (See Fig. 10)

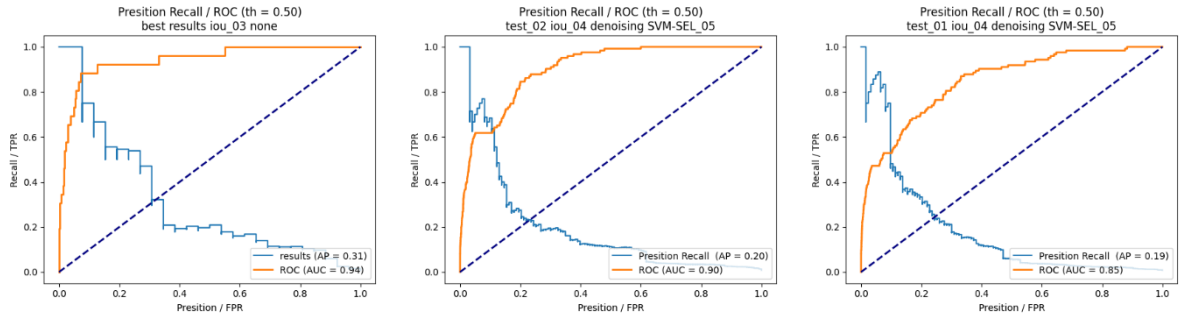


*Figure 10: Precision vs Recall curves (blue) and ROC curves for different features extractions and ROIs enhancements.*

# VII- Annex 1: Basic optical disk removal

As mentioned earlier, the optical disk (OD) region was removed to avoid distortions in image preprocessing. This is because the OD is one of the brightest areas of the eye, and since Soft Exudates (SEx) have a similar characteristic, it could generate false positives or hinder precise differentiation between that region and the Sex. Additionally, by removing the OD region, the complexity of the image is reduced, and regions that are not of interest to the model's objective are eliminated.

The procedure followed to accomplish this is based on the fact that the OD:
1. Is almost always the brightest area in the image
2. Is circular

Considering these characteristics, two main steps were performed:
1. Image preprocessing
2. Candidates detection

## 1. Image preprocessing

### *Step 0: Reduce the image size*

The image was reduced to 10% of its original size. Since we are not performing an exhaustive segmentation of the OD, there is no problem with losing "fine" information when taking this action. Additionally, it helps eliminate some amount of noise and accelerates the following steps.

### *Step 1: Change the color space of the image to HSV and extract the Value channel (V)*

The color space is changed to HSV, and the V channel, which contains information about the image's value (or brightness), is extracted. Based on the previously mentioned first characteristic, the OD stands out significantly in this channel.

### *Step 2: Apply CLAHE*

CLAHE was applied to the extracted channel to enhance contrast while limiting noise amplification. The clip value used varies depending on the average intensity of the image. Brighter images had a higher clip value (*clahe_clip = 6*) compared to darker images (*clahe_clip = 1*). This difference is due to the need to avoid aggressive clipping in brighter images to prevent the loss of relevant information. On the other hand, it is more beneficial to limit contrast in darker images to avoid artifacts or distortions.

### *Step 3: Apply a binary threshold*

After applying CLAHE, the image was binarized using a relatively high threshold (th = 205) since (as mentioned earlier) the OD region stays due to its high brightness.

### *Step 4: Apply an opening*

Finally, a binary opening operation was performed to eliminate noise caused by other bright areas in the image. The opening operation was done using a circular SE with a radius of 10 since the OD represents a considerably large area of the image, it wouldn't be lost during this operation.

## 2. Candidates detection

### *Step 5: Select the best candidate*

Two approaches were used for candidate detection: *minimum bounding circles* and *Hough circles*. The circle corresponding to the OD was chosen afterward.

#### Minimum bounding circles candidates:

These candidates were chosen by creating a circle that encloses the contour with the largest area in the binary image.

#### Hough circles candidates:

These candidates were selected using *Hough circles* and excluding the ones with a radius smaller than 15 (considered noise) or larger than 40 (as no OD is that large in the rescaled image).

#### Combination:

To select the final circle, the following procedures were followed:

- If the centers of the candidates are far apart or the image is very bright:
  The Hough circles candidate is chosen.
  - If the centers are far apart, the second characteristic of the OD is considered, and in this case, the candidates obtained with Hough circles represent better this characteristic. See *Fig. 13A*
  - If the image is very bright, the candidates based on minimum bounding circles include a lot of noise around the OD and tend to capture very large regions. The circles produced by Hough circles are more reliable in such cases. See *Fig. 13B*
- If not:
  In this case, both candidates represent the OD quite well. Therefore, a circle is created by averaging the two candidates' parameters to preserve information from both candidates. See *Fig. 13C*

The final result of this step can be the circle obtained, or a rescaled contour of that same circle.

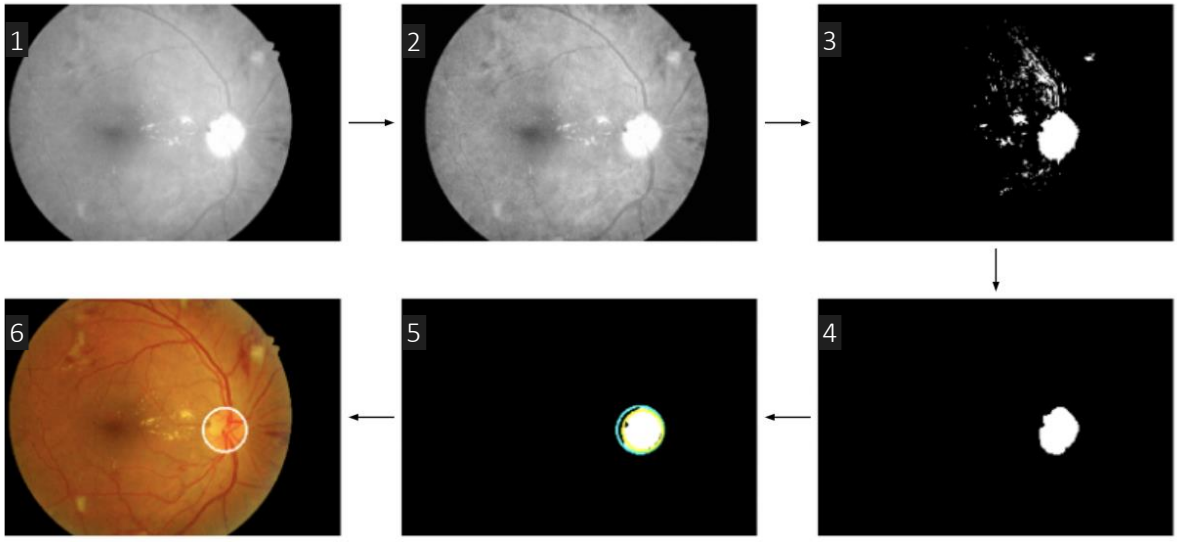


*Figure 12: Steps to detect the region of the OD and the region chosen*

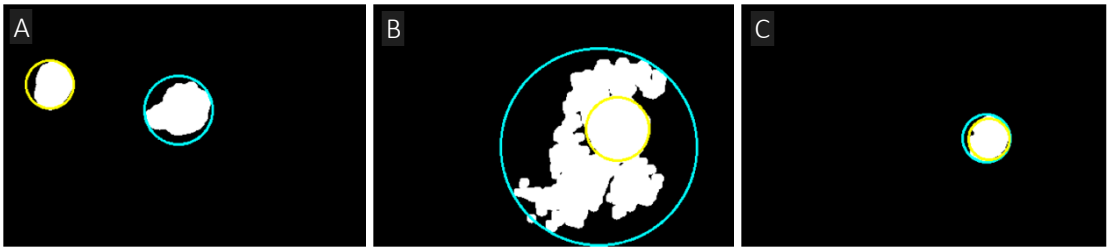


*Figure 13: Image of the candidates to the OD: hugh circles → Yellow, Minimum bounding circle → cyan*

# VIII- Annex 2: Advance optical disk removal:

This approach follows the Basic OD detection algorithm, and it aims to accurately detect and remove the optic disc region from retinal images, allowing for improved exudate detection.

## *Steps 1-2: Obtain ROI from basic OD removal algorithm and apply a circular mask to it*

This circular mask is used to focus the analysis on the OD region.

## *Step 3: The space color of the image is changed to HSV, and the V channel is extracted*

As stated before, by extracting the V channel, the contrast between the OD and the background is enhanced.

## *Step 4: Gamma correction with sigma depending on the mean intensity*

In this step, the mean intensity of each ROI was calculated, then a gamma correction was applied in function to that mean intensity. This adjustment modified the parameter of $sigma$ as follows:

- If the mean intensity is less than 150, $\mathrm{sigma} = 66$.
- If the mean intensity is greater than 190, $\mathrm{sigma} = 0.01$.
- Otherwise, $\mathrm{sigma} = -0.000061 * mean\_intensity^2 + 0.0167 * mean\_intensity - 0.8678$

These values were derived through a regression analysis, correlating sigma with the "quality" of the lesion segmentation.

## *Step 5: Median blur*

Median blur with kernel size = 51 was done to reduce noise, smooth uneven regions, and enhance edge information.

## *Steps 6-8: Thresholding and Binary morphology*

First, an Otsu thresholding technique was applied to the image to convert it into a binary form. Next, two binary morphology operations were performed:

- An opening operation using a structuring element (SE) of size 55 x 55. This step aimed to remove noise while retaining the OD since it is relatively large.
- A closing operation using a SE of size 55 x 55. This step ensured that the OD region does not contain any "holes" or gaps.

## *Step 9: Select the best candidate with area and circularity*

Contours are extracted, and the contour with the highest area is chosen as the OD region. If the circularity of the chosen contour does not meet the minimum circularity threshold, the Hugh circles algorithm is again used to detect a circular OD.

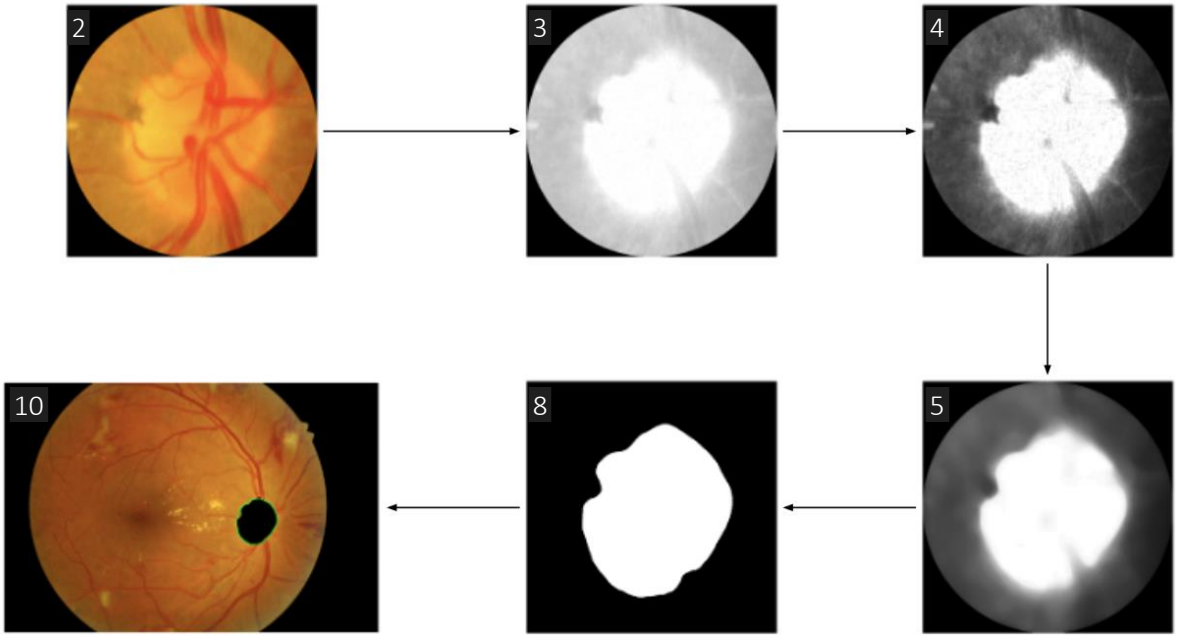


*Figure 14: Steps followed to detect the OD*

Finally, the candidate detected as the OD was compared with the groundtruth to evaluate the performance of this segmentation. This was evaluated with respect to the dice coefficient pixel by pixel ($D_{OD} = \frac{2*TP}{2*TP+FP+FN}$), the result obtained was a $D_{OD} = 0.93$ indicating a well-segmented OD.

# References


[1] Wan, C., Chen, Y., Li, H., Zheng, B., Chen, N., Yang, W., Wang, C., & Li, Y. (2021). EAD-Net: A Novel Lesion Segmentation Method in Diabetic Retinopathy Using Neural Networks. Disease Markers, 2021, 1–13. https://doi.org/10.1155/2021/6482665

[2] Santos, C., Aguiar, M., Welfer, D., & Belloni, B. (2022). A New Approach for Detecting Fundus Lesions Using Image Processing and Deep Neural Network Architecture Based on YOLO Model. Sensors, 22(17), 6441. https://doi.org/10.3390/s22176441

[3] Zhang, X., Thibault, G., Decencière, E., Marcotegui, B., Laÿ, B., Danno, R., Cazuguel, G., Quellec, G., Lamard, M., Massin, P., Exudate, al, ere, E., La, B., Chabouis, A., Victor, Z., & Erginay, A. (2014). Exudate detection in color retinal images for mass screening of diabetic retinopathy. Medical Image Analysis, 18(7). https://doi.org/10.1016/j.media.2014.05.004ï

[4] Patel, P. S., & Sadda, S. R. (2013). Retinal Artery Obstructions. In Retina (pp. 1012–1025). Elsevier. https://doi.org/10.1016/B978-1-4557-0737-9.00051-5

[5] Bindu, S., Prudhvi, S., Hemalatha, G., Raja Sekhar, N., & Nanchariah, M. v. (2014). Object Detection from Complex Background Image Using Circular Hough Transform. In Journal of Engineering Research and Applications www.ijera.com (Vol. 4, Issue 4). www.ijera.com

[6] Fraz, M. M., Jahangir, W., Zahid, S., Hamayun, M. M., & Barman, S. A. (2017). Multiscale segmentation of exudates in retinal images using contextual cues and ensemble classification. Biomedical Signal Processing and Control, 35, 50–62. https://doi.org/10.1016/j.bspc.2017.02.012

[7] Friedman, N. J., & Kaiser, P. K. (2018). Posterior Segment. In Case Reviews in Ophthalmology (pp. 251–312). Elsevier. https://doi.org/10.1016/B978-0-323-39059-0.00006-X

[8] Imani, E., & Pourreza, H.-R. (2016). A novel method for retinal exudate segmentation using signal separation algorithm. Computer Methods and Programs in Biomedicine, 133, 195–205. https://doi.org/10.1016/j.cmpb.2016.05.016

[9] Porwal, P., Pachade, S., Kokare, M., Deshmukh, G., Son, J., Bae, W., Liu, L., Wang, J., Liu, X., Gao, L., Wu, T., Xiao, J., Wang, F., Yin, B., Wang, Y., Danala, G., He, L., Choi, Y. H., Lee, Y. C., … Mériaudeau, F. (2020). IDRiD: Diabetic Retinopathy - Segmentation and Grading Challenge. Medical Image Analysis, 59, 101561. https://doi.org/10.1016/j.media.2019.101561

[10] Ünver, H., Kökver, Y., Duman, E., & Erdem, O. (2019). Statistical Edge Detection and Circular Hough Transform for Optic Disk Localization. Applied Sciences, 9(2), 350. https://doi.org/10.3390/app9020350